

WAKE/BOUNDARY-LAYER INTERACTIONS IN TWO AND THREE DIMENSIONS

by L.C.Squire, D.Agoropoulos and A.H.Kh.Moghadam

Cambridge University Engineering Department

Abstract

This paper describes a programme of work on the interaction between wakes and boundary layers which occurs on multi-element aerofoils in high lift situations. The work has concentrated on the following two aspects: (a) experiments designed to isolate the separate effects of slat shape, gap size, wake strength, pressure gradient and crossflow and (b) the careful evaluation of various numerical schemes for predicting these flows. It is shown that in two-dimensional flow the turbulence levels in the wake and the pressure gradients on the main aerofoil are the main parameters governing the interaction process and that these effects can be predicted with good accuracy by numerical calculations incorporating either an algebraic stress model or a K-epsilon model.

The work on three-dimensional aspects of the interaction has not reached such an advanced stage but a digital system for measuring and recording all the components of the Reynolds stress tensor using a triple hot-wire probe has been developed and used to measure a number of three-dimensional flows. In cases where the flow is quasi-three-dimensional, (that is it resembles the flow over an infinite yawed wing) the numerical calculations can be used to predict the streamwise and crossflow velocities with similar accuracy to that achieved in two dimensions.

1 Introduction

In the flow over multi-element aerofoils the wake from one element flows back over the upper surface of the element immediately downstream and an interaction takes place between the flow in the wake and the boundary layer on the downstream element. Tests on multi-element aerofoils and wings have shown that when the slat and flaps are deployed in the optimum configuration the interaction between the wing wake and the flap boundary layer is relatively weak. However, that between the slat wake and the boundary layer on the main wing is very strong. Furthermore it has been found that the accurate calculation of this interacting flow is a necessary step in the prediction of the flow about the whole aerofoil. This is particularly true in high-lift conditions where the boundary layer on

the upper surface of the main portion of the aerofoil is often on the point of separating.

Recently a number of studies have been made of the flow around fairly realistic aerofoil configurations with slat and flaps^{1,2,3}. Although these results are very useful in giving a general view of the overall flow around multi-element aerofoils they are very complicated and therefore are not very useful in building up a physical picture of the various interaction processes. Furthermore they are not particularly useful for testing different turbulence models since the complexity of the flow makes it difficult to find the source of the discrepancies which inevitably occur between experiment and prediction.

To overcome these difficulties a programme of work has been carried out in the Aerodynamics Laboratory at Cambridge with the object of setting up a number of simple interacting flows which would allow the effects of various parameters (such as turbulence levels in the wake, pressure gradient or crossflow) on the interaction to be isolated and understood. Initial tests were made in a special boundary-layer tunnel (see Fig 1) on the interaction between the wake from a relatively thick aerofoil and a fully developed turbulent boundary layer on a flat plate and the separate effects studied included gap size (the distance between the aerofoil and the flat surface), aerofoil lift, and imposed pressure gradient in the interaction region. Although these tests cast some light on the interaction processes the actual interaction was dominated by vortices shed by the thick aerofoil and so the interaction was unrepresentative of practical configurations. Thus in the second stage of the work a circulation control model was designed and tested. It consisted of an elliptic section together with a realistic sharp-keeled slat. By a suitable combination of incidence, tangential blowing and slat position a satisfactory leading edge flow with suction peaks of $C_p = -5$ was achieved. Measurements of surface pressures on the ellipse and pitot traverses in the confluent flow of the slat wake and the ellipse boundary layer were then used to set up a number of simple, but realistic, interacting flows in the boundary layer tunnel. In all 5 different configurations were tested in the boundary layer tunnel but results from only one of them are considered in this paper.

Three-dimensional effects were studied in the interaction region by sweeping the aerofoil used to produce the wake. Thus the results presented correspond to the interaction of a three-dimensional wake with a boundary layer which is two-dimensional when undisturbed. Fuller details of this investigation are presented in Ref. 4.

2 Experimental Details

The main experiments were made in a special boundary-layer tunnel in the Aerodynamics Laboratory of Cambridge University Engineering Department. This tunnel has a test section of about 2m length and a cross section of 1.5m x 0.3m. All tests were made at a free stream velocity of 13m/s with a corresponding turbulence level of about 0.2%. The roof of this tunnel was made of perforated plate and by adjusting the porosity of this plate and by adding a gauze resistance at the tunnel exit any desired pressure gradient could be imposed along the tunnel.

The test boundary layer developed on the bottom wall of the tunnel which was made of highly polished aluminium alloy. This wall was provided with a large number of removable plugs so that probes could be traversed through the viscous layer at close intervals. To ensure that the test boundary layer was fully turbulent a trip wire was placed 0.8m upstream of the first measuring position. For the results reported here traverses through the boundary layer were made at intervals of 203mm that is about 12 thicknesses of the initial undisturbed boundary layer. In most cases the first traverse was made about 200mm downstream of the trailing edge of the model producing the wake.

The wakes were generated by one of two models, one a 38% thick strut and the other a 15% symmetric aerofoil. Either model could be mounted at any vertical distance above the test surface. For all tests the models spanned the full width of the tunnel. For the two-dimensional tests the models were mounted normal to the stream direction, while three-dimensionality was introduced by sweeping the model at angles up to 40°.

Measurements of the mean velocities U , V and W and the Reynolds stresses u^2 , v^2 , w^2 , $-uv$, $-uw$, $-vw$ were obtained by means of linearised hot wires. Disa X-wires being used for the two-dimensional layers and a Disa triaxial probe for the three-dimensional layers. For all the measurements standard anemometers and linearisers were used and, after filtering, the signals were digitised and processed by computer. The accuracy of the whole system is illustrated by the results presented in Figs. 2, 3 and 4. Thus Fig. 2 compares values of the mean velocity U measured by the X-wire and by a standard pitot tube. Fig. 3 compares profiles of the normal stress u^2 measured by the X-wire using the digital system and the corresponding results obtained from a single hot-wire using a conventional analogue

system. (Since it was not possible to measure profiles at exactly the same station with the single and X-wire probes, the single wire results are compared with X-wire results obtained just upstream and just downstream). As will be seen the agreement between the results presented in Figs 2 and 3 is excellent. Comparison of results obtained by the X-wire (in the horizontal and vertical planes) with results obtained with the triple wire probe are shown in Fig. 4. The agreement between the results for the mean velocities obtained by the two types of probe is very good with all the results agreeing to within plotting accuracy. However, the agreement in the values of the normal stresses v^2 and w^2 and in the shear stress uv near the wall is poor. It is thought that this discrepancy is associated with spatial resolution since the three active wires of the triple wire probe occupy a sphere of 3mm diameter whereas the two active wires of the X-wire probe are confined to a sphere of diameter 1.2mm. Thus one might expect errors from the triple wire probe in high gradient regions. The accuracy of the whole digitization system was checked by a number of independent methods including the development of two separate programs for the analysis of the data. From these checks it is estimated that the maximum error in the Reynolds stresses is better than 10% of their respective maximum value, except near the wall where the error may rise to 15%. However, the maximum error in any of the components of the mean flow is estimated to be less than 2% of the free-stream velocity.

3 Numerical Methods

All the calculated results shown in this paper were calculated by an enhanced version of a computer code developed at Manchester Institute of Science and Technology. Two second order turbulence models are incorporated into the code: a K-epsilon model and an algebraic stress model. Both models use wall laws to bridge the near-wall viscous region.

During the present work the following extensions have been included in the code.

(1) An allowance for the effects of small departure from two-dimensionality by adding a term DU to the continuity equation. This correction assumes that the lack of two-dimensionality is due to simple convergence or divergence of the flow; that the velocity profiles are collinear, and that the divergence D is constant through the viscous layer and can be obtained from the out-of-balance term in the two-dimensional momentum integral equation.

(2) The inclusion of additional terms in the x-momentum equation to allow for the normal stress and for the variation of pressure across the layer. This modification was only used with the algebraic stress model since this model gave values of u^2 and v^2 directly. Values of u^2 and v^2 can be obtained from the K-epsilon model by assuming an isotropic eddy viscosity, however, as shown below, the values obtained are not very accurate.

(3) The solution for the spanwise velocity in cases where the chordwise and spanwise flows could be assumed to be independent. This solution was only obtained using the K-epsilon model and the corresponding shear stress was calculated by assuming an isotropic eddy viscosity.

4 Results

4.1 Thick aerofoil results

As mentioned in the introduction initial tests were made on the interaction between the wake from a relatively thick strut and the turbulent boundary layer on a flat surface to determine the separate effects of gap size, pressure gradient etc.. Typical results are presented in Figs. 5(a) and 5(b). Fig. 5(a) shows the mean-flow profile immediately downstream of the trailing edge of the thick strut and profiles at two stations in the interaction region. Station 4 is approximately 50 initial boundary-layer thicknesses downstream of station 0 and station 6 is about 20 initial boundary-layer thicknesses further downstream. In the figure the open symbols represent results obtained in an interacting flow in nominally zero pressure gradient, while the solid and dashed lines correspond to results measured in the undisturbed boundary layer and in the undisturbed wake respectively. From this figure it can be seen that at the initial station in the interacting flow the velocity in the potential core is slightly greater than in the free stream but otherwise the flows in the wake and in the boundary layer are identical to those in the undisturbed case. By station 4 the interaction appears to have just produced a smooth fairing between the undisturbed wake and undisturbed boundary layer. Close inspection, however, shows that the interaction has affected the whole of the inner half wake and the outer half of the boundary layer. The effect of the application of an adverse pressure gradient between stations 4 and 6 appears to produce a more marked interaction in the mean flow (solid symbols in Fig. 5(a)). However, this is mainly due to the sudden increase in thickness of the undisturbed boundary layer and to the fact that the wake centreline moves away from the wall so that the interaction still only affects the inner half of the wake. The extent of the interaction is confirmed by the corresponding shear stress profiles presented in Fig. 5(b).

These results were of interest in defining the main parameters governing the interaction, however, they were unrealistic in the sense that the flow in the wake was dominated by vortex shedding. This led to extensive regions in the interaction where the shear stress was of opposite sign to the velocity gradient (that is the "eddy viscosity" was negative). Also the pressure gradients used were not applied at the beginning of the interaction. Thus in the next series of tests the aerofoil producing the wake was much thinner (15% compared with 38%) and the pressure gradient was matched to those that are likely to occur on practical wings.

4.2 Circulation control model and the resultant interaction

In order to provide data on realistic pressure distributions a circulation control model was designed and tested in a conventional low speed wind tunnel. This model consisted of an elliptic main element together with a realistic sharp-heeled slat. High lift coefficients were achieved by means of tangential blowing into the upper surface boundary layer near the trailing edge of the ellipse. Several incidences and blowing rates were tried until a satisfactory leading edge flow with a realistically high suction peak of $C_p = -5$ was achieved. With this configuration some pitot traverses were made in the confluent viscous flow on the upper surface of the ellipse downstream of the slat. These results (not shown here) were then used as a guide for the measurements in the boundary layer tunnel.

For the tests in the blower tunnel the pressure gradient along the test section was adjusted so that a non-dimensional pressure gradient parameter matched that measured on the circulation control model. While an asymmetrical wake similar to that found in that model was obtained by adding a small fence on the lower surface of the aerofoil to create a separation bubble. Typical results for the boundary layer development are presented in Fig. 6 where the measured development of the mean velocity, the turbulent kinetic energy and the Reynolds shear stress are compared with calculated developments obtained by use of the two turbulence models described above. Full details of all these boundary-layer measurements together with measurements made in interactions without an adverse pressure gradient and in interactions with larger and smaller separation bubbles are given by Agoropoulos in ref. 8.

Before considering the results of Fig. 6 in detail it should be noted that the measured momentum thickness increased less rapidly than required to satisfy the momentum integral equation (Fig. 7). This corresponds to a slight divergence of the flow and, as indicated above in section 3, this divergence has been included in the calculations. In general the agreement between theory (corrected for divergence) and experiments shown in Fig. 6 is reasonable. The calculated mean velocity profiles have the correct shape but tend to be rather smoother than the measured profiles towards the downstream end of the interaction. In part this is because the divergence is not necessarily constant (collinear) through the confluent layer so the correction is only approximate at the downstream end of the tunnel. However, in all the results obtained there was a definite tendency for both turbulence models to over predict the decay of the wake and the core flow, that is the calculated profiles were always smoother than the measured profiles.

This is illustrated in Fig. 8 where a full set of measured and calculated results are presented for the last measured station for a constant pressure interaction downstream of a symmetric aerofoil. This flow was measured using the triple wire probe and is known to be

accurately two-dimensional so errors must be associated with the turbulence models. Again the measured mean velocity profile shows a less rapid merging of the wake and the boundary layer than is shown by both turbulence models. This trend is also clear in the corresponding shear stress profile, where the prediction using the K-epsilon model is slightly more accurate. In the results for the corresponding normal stresses and for the turbulent kinetic energy it can be seen the turbulent kinetic energy and the normal stress u^2 are both best predicted by the algebraic stress model. The results for v^2 and w^2 are less conclusive. However, remembering that the results presented in Fig. 4 suggest that these quantities as measured by the triple probe are too large, it would appear that the values given by the algebraic stress model are reasonable, whereas those from the K-epsilon model (using an isotropic eddy viscosity) are clearly inadequate.

Along the centreline of the wake, where, in adverse pressure gradients, the difference between the production and dissipation of turbulent kinetic energy is large and increases under flow deceleration, the algebraic stress model predicts the mean velocity U more accurately than the K-epsilon model. Both models underestimate the expansion of the confluent layer along the free stream boundary as shown by the mean velocity profiles and the Reynolds stresses. This is hardly surprising given the use of closures based on time-averaged, fully-turbulent flows. Improvement could be obtained by prescribing a suitable intermittency distribution but this has not been attempted here.

4.3 Results with crossflow

As mentioned in the introduction the effect of crossflow on the interaction was studied by sweeping the aerofoil used to produce the wake. With the aerofoil at zero, or positive, incidence the three-dimensionality in the interaction region was small even when the aerofoil was swept at 40° . Eventually it was found that the only way to produce significant crossflow in a simple way was to place the aerofoil at a negative incidence of 3° at a sweep of 40° . Thus the interaction is artificial in the sense that the slat lift is negative. However, it was felt that the flow so produced is of interest in that the wake is asymmetric and there are significant three-dimensional effects in the interaction region. Thus it should provide a useful test case for the calculation methods.

The results presented here were measured along the centreline of the tunnel and check tests off the centreline showed that the flow was virtually independent of spanwise position. Thus the results presented correspond to infinite swept wing conditions. Fig. 9 presents the magnitude and direction of the measured velocity in the interaction region and shows that the general form of the interaction is not greatly affected by the three-dimensional effects. This might be expected since the crossflow angle is relatively small except near the wall in the inner boundary layer. It is also clear that the three-dimensional effects decay rapidly away from the aerofoil so that at approximately two chords downstream of the

trailing edge (station 1) the maximum crossflow in the wake is less than 4 degrees. A similar rapid decay was found by Cousteix and Pailhas¹⁰ in a study of an isolated wake and in a corresponding study of an isolated wake made in the course of the present work. (Since the crossflow in the wake depends on the pressure distribution on the aerofoil the velocity defect and turbulence structure in the isolated wake is not exactly the same as that in the wake at the beginning of the interaction). This rapid decay of the crossflow has important implications for interaction studies since it means that in many cases the three-dimensionality in the wake will be greatly reduced before the main interaction starts.

Fig. 10(a) compares the measured and calculated velocity components in the undisturbed direction, that is the component along the tunnel centreline. The calculations being made by using the two-dimensional program so that all crossflow effects are neglected. As can be seen the agreement between the calculated and measured values is similar to that found in the corresponding two-dimensional case (Fig.8) with, again, the calculated profiles being smoother than those measured. (Note that in Fig.10 and in all the following figures results are only presented for stations 0, 3 and 6.) The agreement between the measured and calculated turbulent quantities is generally less good than in two-dimensions with significance differences within the boundary layer where the crossflow is large. Even in the wake and in the outer part of the boundary layer where the crossflow is small there are important differences (see Figs. 12 and 13, below) with very little to choose between the calculations based on the two turbulence models.

Clearly these differences may be associated with three-dimensional effects, but this could not be checked directly as a full three-dimensional program was not available. However, as the flow was known to be almost independent of the spanwise variable it was decided to calculate the flow by assuming that the flow in the spanwise and chordwise directions were independent. In this case the mean flow in the chordwise direction is given by the solution of the two-dimensional equation and it is a relatively easy matter to modify the computer program to give the solution in the spanwise direction. Measured and calculated profiles for the mean velocity component in the chordwise direction are presented in Fig. 10(b). As will be seen the agreement is now much better than in Fig. 10(a) with excellent agreement between the measured and calculated profiles at the final station. The corresponding profiles for the mean crossflow velocity are shown in Fig. 11, and the agreement between the measured and calculated results is excellent.

As mentioned above the agreement between the measured and calculated turbulent quantities was less good than in the corresponding two-dimensional case. Thus a comparison of the measured values of uv with those calculated by assuming that the flow in the undisturbed direction was two-dimensional showed a similar trend to that illustrated in Fig. 8. That is the calculated stress is too high in the interaction region. On the other hand the calculated values of uv in the chordwise direction were much lower than

the measured values in the boundary layer. However, in the wake the agreement between the measured values and those calculated using the K-epsilon model was excellent.

Measured and calculated values for the turbulent kinetic energy are shown in Figs 12(a) and 12(b), while results for the normal stress u''^2 in the isolated wake are shown in Figs. 13(a) and 13(b). In these figures the results in the chordwise direction are normalised by the corresponding free-stream velocity component in the chordwise direction (U_{e1}) and the difference in the experimental results for K in Figs. 12(a) and 12(b) is purely due to this normalisation. From these figures it is clear that the prediction of the turbulent kinetic energy by use of the two-dimensional equation in the stream direction produces results which are in reasonable agreement with the measurements. Furthermore there is very little difference between the results from the two turbulence models. On the other hand the calculations in the chordwise direction under predict the level of the kinetic energy in the boundary layer. In all cases the predicted values for the normal stress u''^2 are too high in the isolated wake and similar results were found for the interacting flow.

5 Conclusions

(a) The two-dimensional results show that the overall flow in the interaction can be calculated with reasonable accuracy by use of an algebraic stress model and with slightly less accuracy by use of a K-epsilon model. However, it should be noted that the comparisons presented here do not include the effects of surface curvature and the inclusion of these effects may require further work. Also all the calculated results used in the comparisons presented here started from measured profiles downstream of the trailing edge. In a full calculation it would be necessary to obtain these initial profiles from the calculated flow around the slat.

(b) The main point of interest from the experiments with the swept wake is the rapid decay of the crossflow downstream of the trailing edge. In fact in the experiment it was extremely difficult to generate an interacting flow with significant three-dimensional effects and the flow finally used is slightly artificial. Comparisons of the measured and calculated results for this flow shows that the mean flow can be predicted with similar accuracy to that achieved in the two-dimensional case. However, the prediction of the turbulent quantities is less satisfactory. However, the calculations considered here were not fully three-dimensional so some of the disagreement may be due to the numerical scheme used in the calculations, rather than to inadequacies in the turbulence models.

Acknowledgments

During the course of this work D. Agoropoulos was supported by grants from Corpus Christi College and British Aerospace P.L.C. and A.H.Kh.Moghadam was supported by a research studentship from Trinity College. The authors wish to thank these bodies for their support.

References

1. Bario F., Charnay G., Papailiou K.D. "An Experiment Concerning the Confluence of a Wake and a Boundary Layer", Trans. ASME, J. Fluids Engineering, vol.104, pp. 18-24, 1982.
2. Brune G.W., Sikavi D.A. "Experimental Investigation of the Confluent Boundary Layer of a Multielement Low Speed Aerofoil", AIAA Paper 83-0566, 1983
3. Braden J.A., Whipkey R.R., Jones G.S., Lilley D.E. "Experimental Study of the Separating Confluent Boundary-Layer", NASA CR 3655, 1983
4. Moghadam A.H.Kh., Squire L.C. "Three-dimensional interaction of wakes and boundary layers". AIAA Paper 86-1820-CP, 1986.
5. Launder B.E., Spalding D.B. "The numerical computation of turbulent flow", Computer methods in Applied Mechanics and Engineering Vol.3 pp. 269-289, 1974.
6. Launder B.E., Reece G.J., Rodi W. "Progress in the development of a Reynolds stress turbulence closure", Jour. Fluid Mech. Vol 68 pp. 537-566, 1975.
7. Zhou M.D., Squire L.C. "The Interaction of a Wake with a Turbulent Boundary Layer", Aeronautical Jour. Vol.89 pp. 72-81, 1985
8. Agoropoulos D. "Interactions between Wakes and Boundary Layers". Ph.D. Dissertation, University of Cambridge, 1986
9. Patel V.C., Scheuerer G. "Calculation of Two-Dimensional Near and Far Wakes", AIAA J. vol.20, pp. 900-907, 1982
10. Cousteix J., Pailhas G. "Three-dimensional wake of a swept wing", Symposium on Structure of Complex Turbulent Shear Flow. Springer-Verlag, Berlin. pp 208-218, 1983

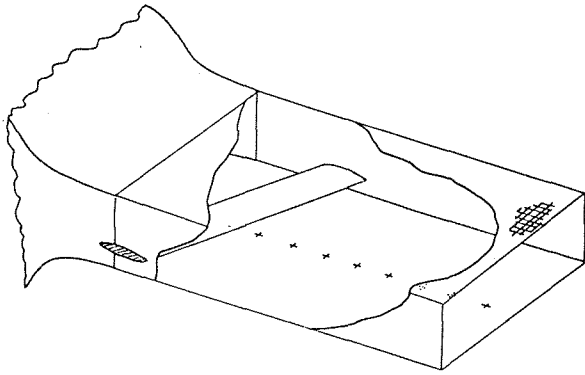


Fig. 1 Sketch of test section

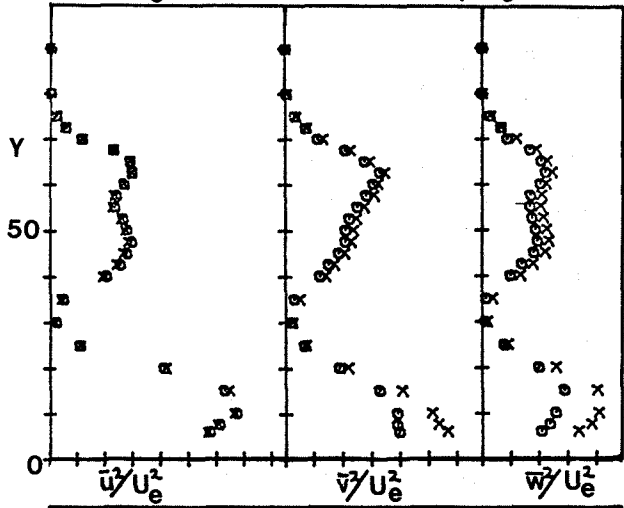
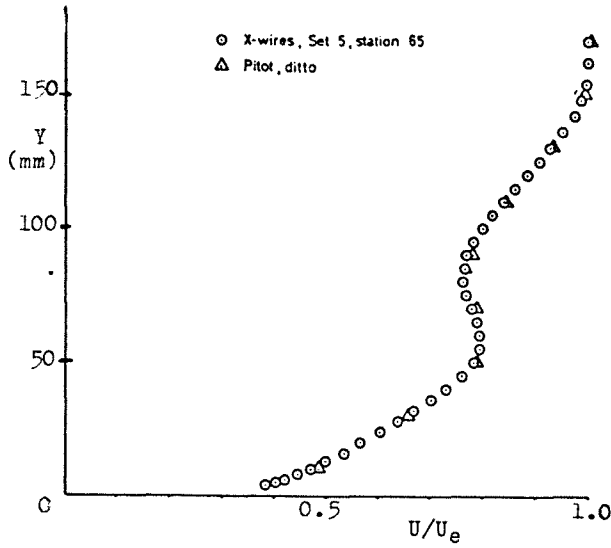
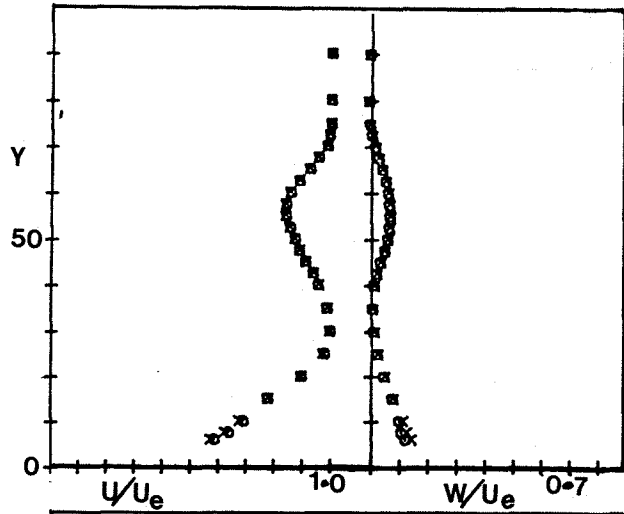


Fig. 2 Comparison of mean velocity as measured by a pitot tube and a X wire.

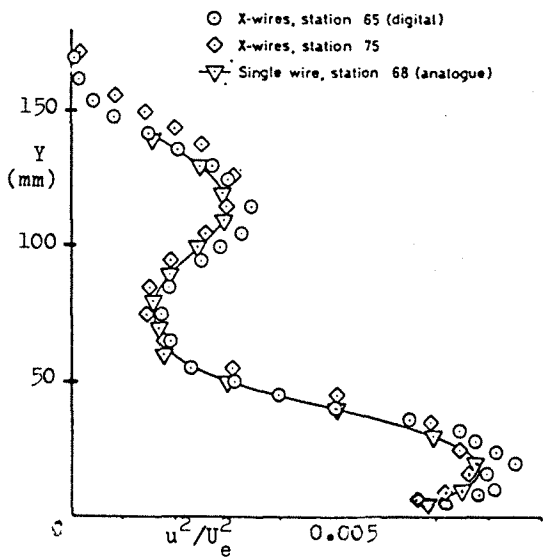


Fig. 3 Comparison of $\overline{u^2}$ as measured by a single wire and a X wire.

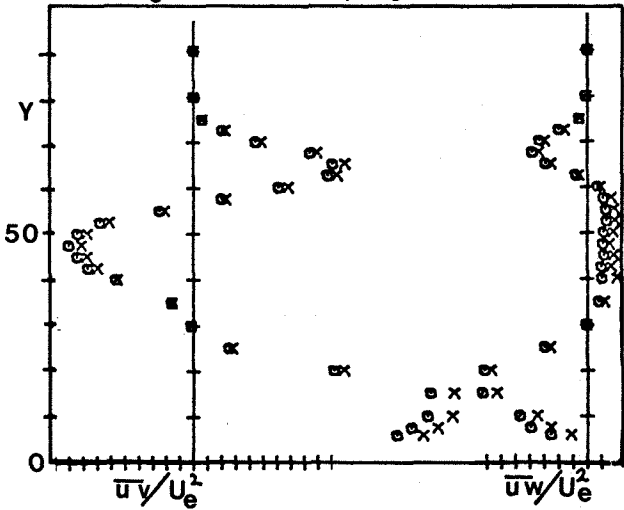


Fig. 4 Comparison of results obtained by the triple wire probe and by X wires. • X wire results; x triple wire results.

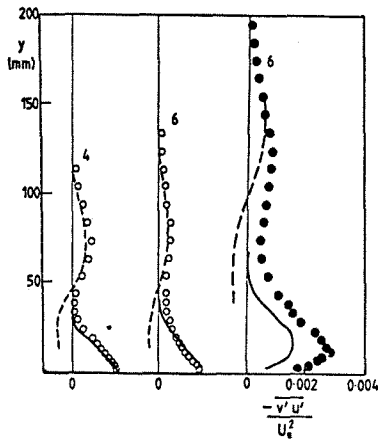
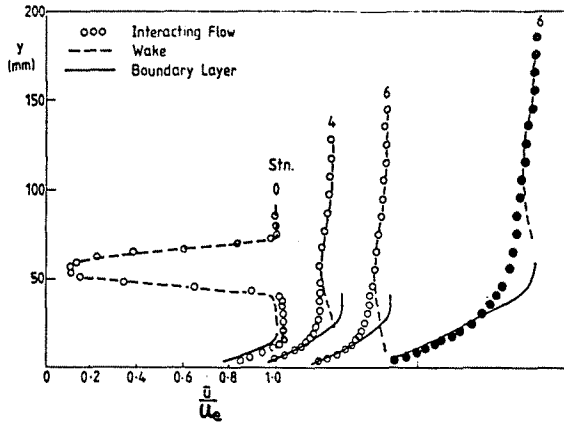


Fig. 5 Mean velocity and shear stress profiles in a simple interaction.

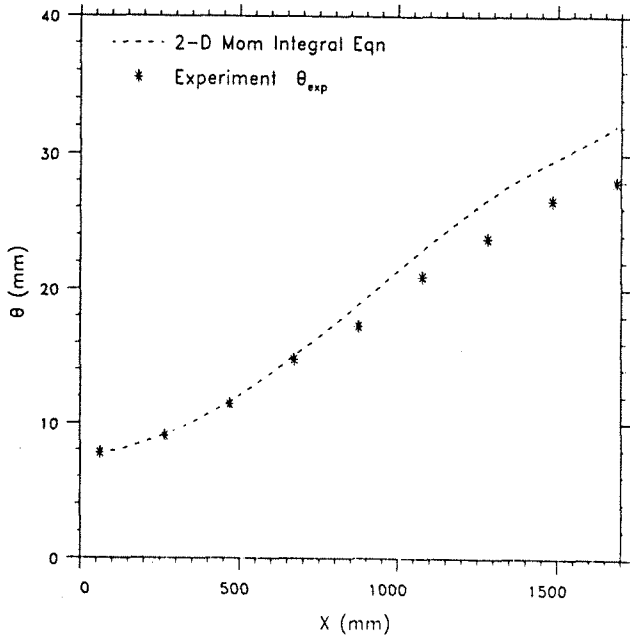


Fig. 7 Momentum balance for the two-dimensional interaction in an adverse pressure gradient. The calculated values of θ were obtained from a numerical solution of the two-dimensional momentum integral equation using measured value for H , c_f and the external velocity distribution.

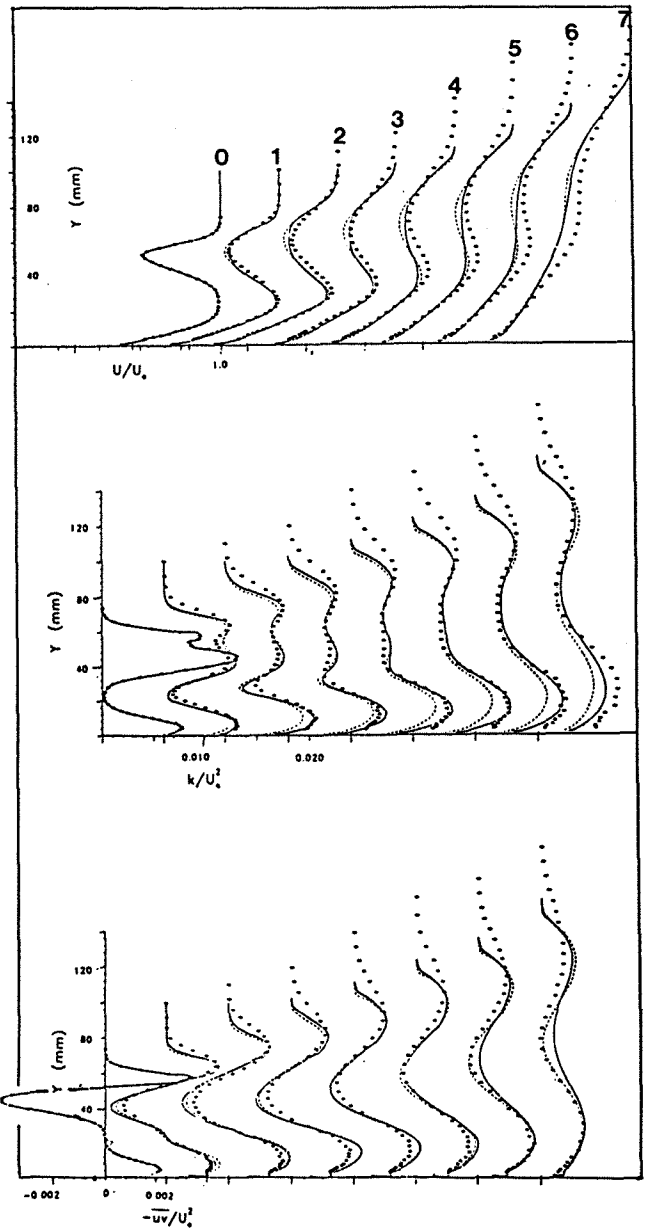


Fig. 6 Mean velocity profiles and turbulence quantities in a two-dimensional interaction with an adverse pressure gradient. \bullet measured points; --- K-epsilon model; — algebraic stress model.

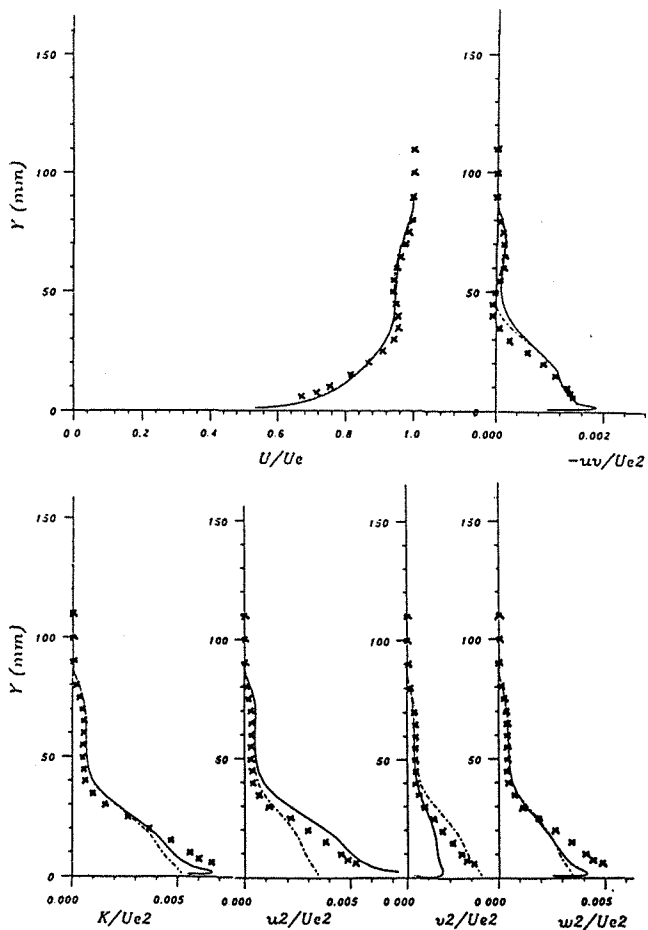


Fig. 8 Measured and calculated profiles at the last downstream station in a two-dimensional interaction in zero pressure gradient. x measured points: ----- K-epsilon model: — algebraic stress model.

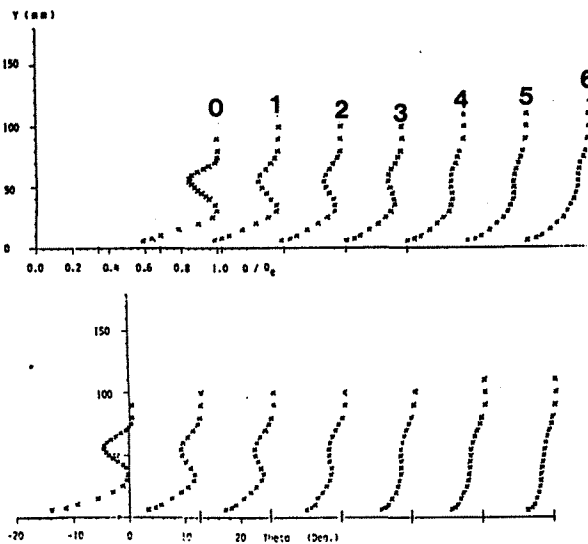


Fig. 9 Magnitude and direction of the measured velocity profiles in a three-dimensional interaction.

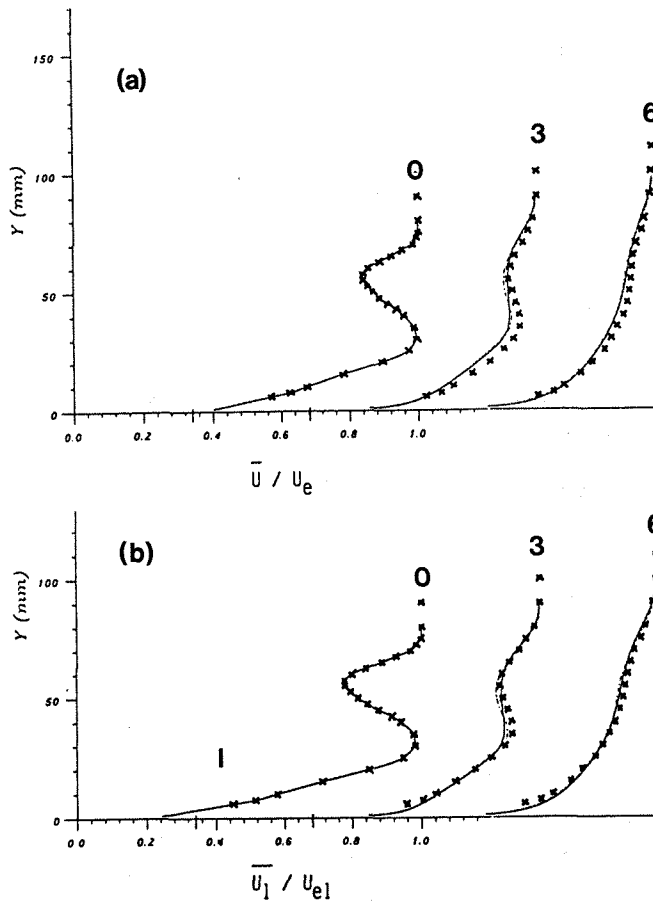


Fig. 10 Measured and calculated velocity components in a three-dimensional interaction. x measured points: ----- K-epsilon model: — algebraic stress model. (a) streamwise calculations: (b) chordwise calculations.

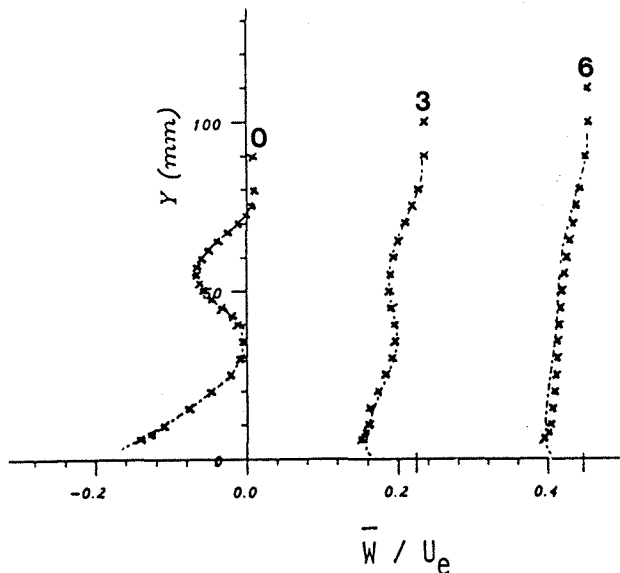


Fig. 11 Measured and calculated velocity components in the crossflow direction in a three-dimensional interaction. x measured points: ----- K-epsilon model:

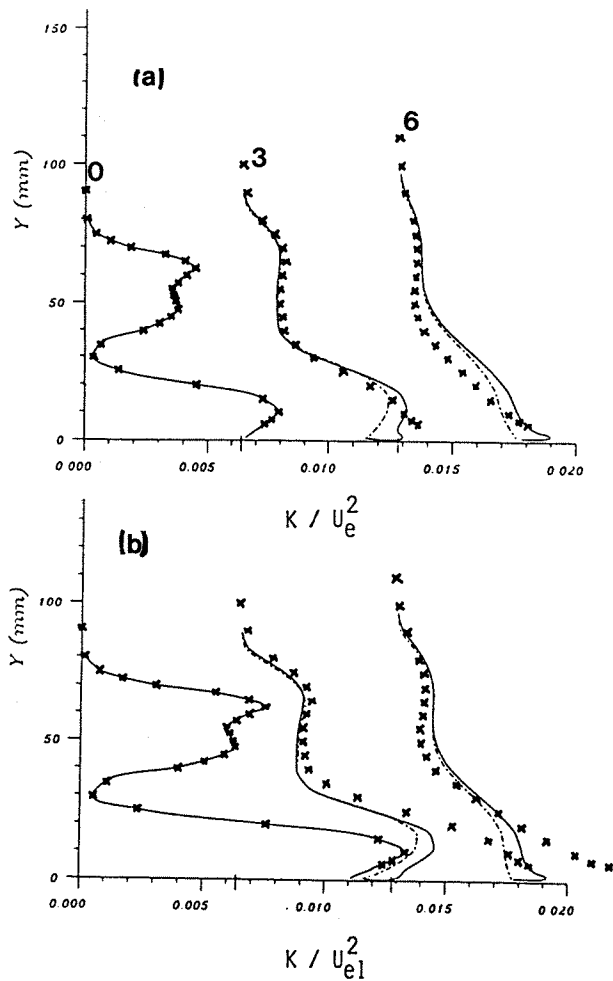


Fig. 12 Measured and calculated turbulent kinetic energy in a three-dimensional interaction. x measured points: ----- K-epsilon model: ——— algebraic stress model. (a) streamwise calculations: (b) chordwise calculations.

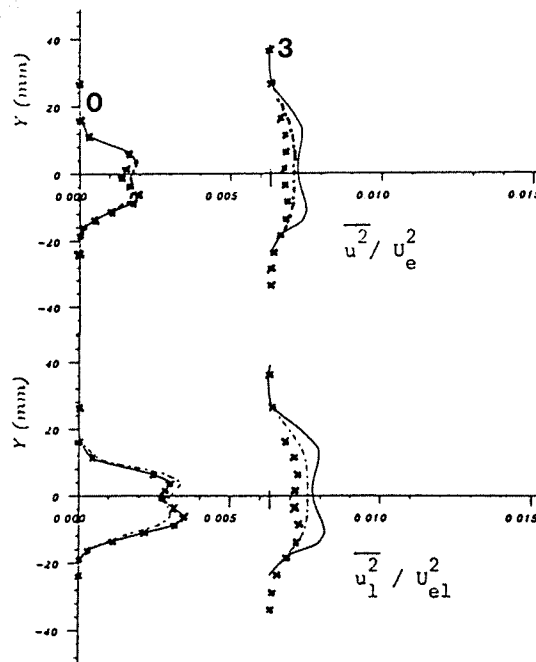


Fig. 13 Measured and calculated normal stress in a three-dimensional isolated wake. x measured points: ----- K-epsilon model: ——— algebraic stress model. (a) streamwise calculations: (b) chordwise calculations.